Recent progress of GEANT4 electromagnetic physics for LHC and other applications

Bagulya, A.; Brown, J. M.C.; Burkhardt, H.; Grichine, V.; Guatelli, S.; Incerti, S.; Ivanchenko, V. N.; Kadri, O.; Karamitros, M.; Maire, M.

DOI
10.1088/1742-6596/898/4/042032

Publication date
2017

Document Version
Final published version

Published in
Journal of Physics: Conference Series

Recent progress of GEANT4 electromagnetic physics for LHC and other applications

IOP Conf. Series: Journal of Physics: Conf. Series **898** (2017) 042032 doi:10.1088/1742-6596/898/4/042032

Recent progress of GEANT4 electromagnetic physics for LHC and other applications

A Bagulya[1], J M C Brown[2], H Burkhardt[3], V Grichine[1], S Guatelli[4], S Incerti[5,6], V N Ivanchenko[3,7], O Kadri[8], M Karamitros[6], M Maire[7,9], K Mashtakov[10], M Novak[3], L Pandola[11], P G Rancoita[12], D Sawkey[13], M Tacconi[12,14], L Urban[7]

[1]Lebedev Physical Institute, Moscow 119991, Russia
[2]Delft University of Technology, Radiation Science and Technology, 2629JB Delft, The Netherlands
[3]CERN, 1211 Genève 23, Switzerland
[4]University of Wollongong, Centre for Medical Radiation Physics, Wollongong NSW 2522, Australia
[5]CNRS-IN2P3, CENBG, UMR 5797, F-33170 Gradignan, France
[6]Université Bordeaux, CENBG, UMR 5797, F-33170 Gradignan, France
[7]Geant4 Associates International Ltd., United Kingdom
[8]King Saud University, Riyadh, Saudi Arabia
[9]IN2P3/LAPP, 74941 Annecy-le-vieux, France
[10]University of the West Scotland, Paisley Campus, Paisley, United Kingdom
[11]INFN, Laboratori Nazionali del Sud, I-95123 Catania, Italy
[12]INFN, Milano-Bicocca, Milano, Italy
[13]Varian Medical Systems, Palo Alto, CA 94304, USA
[14]University Milano-Bicocca, Milano, Italy

E-mail: `Vladimir.Ivantchenko@cern.ch`

Abstract. We report on the recent progress within the GEANT4 electromagnetic physics sub-packages. Several new interfaces and models recently introduced are already used in LHC applications and may be useful for any type of simulation. Significant developments were carried out to improve the user interface, develop models of single and multiple scattering, and validate high energy models. Part of these developments are included in the GEANT4 10.2 release and the full set are available in the new version 10.3 of December, 2016.

1. Introduction

Recent developments in standard EM sub-libraries were driven by two main requirements: to improve the accuracy and robustness of EM models for ongoing Large Hadron Collider (LHC) experiments, and to enable the possibility of simulating various designs of Future Circular Collider (FCC) interaction regions and detectors. In the low-energy region, modifications were mostly introduced for more accurate simulation of atomic de-excitations and for development of DNA models and infrastructure. GEANT4 electromagnetic (EM) physics libraries were described in detail in several reviews [1, 2]. In this work we will discuss selected developments and some validation results mainly relevant to the LHC and FCC.

2. EM sub-package infrastructure upgrades

A new concept of EM parameter definition has been implemented, because the old approach showed difficulties in the multithreaded mode. All EM parameters can now be defined in C++ code or user interface (UI). In addition, several new parameters have been added.

Users may now define the lowest energies for tracking of charged particles. These thresholds are different for e^+/e^- and muons/hadrons. At the end of a step, the kinetic energy of a charged particle is checked and if it is below the user-defined threshold, the particle is killed and its remaining kinetic energy is added to the local energy deposition. This approach permitted the removal of similar energy limits, not transparent to users, from some models.

Specific models [2], including photo-absorption ionization (PAI), microelectronics (Micro-Elec), and DNA [3], can be used per geometry region, and the physics configuration of a GEANT4 reference physics list may be used for a specific region (e.g. where higher precision is required, such as a tracker or a specific calorimeter). These new UI commands are:

- */process/em/AddPAIRegion particle myregion PAI*
- */process/em/AddDNARegion myregion DNAtype*
- */process/em/AddMicroElecRegion myregion*
- */process/em/AddEmRegion myregion EMtype*
- */process/em/printParameters*

Here *myregion* is the name of *G4Region*; *DNAtype* is the name of the DNA physics constructor; *EMtype* is the name of an existing EM physics constructor (for example, *G4EmStandard_option4*). It is recommended to first instantiate the physics list, then redefine specific custom parameters. Also, the C++ interface and UI commands are only active for the master thread. The *G4EmProcessOptions* class of the previous scheme still exists in the GEANT4 distribution, but has been deprecated. It should especially not be used in multithreaded mode.

The upper limit of EM models was extended from 10 TeV to 100 TeV to allow for FCC design studies. The increase of this limit means that the EM tables built in the initialisation phase of GEANT4 require about 10% more memory, and a similar increase in CPU time is required for initialisation. However, in a concrete user application this upper limit may be reduced according to the use case in order to reduce CPU of initialisation and allocated memory. Developments of EM physics models described below improve the accuracy of the simulation of EM processes. In particular, LPM suppression and nuclear form-factors are important at the highest energies.

Rare EM processes [4, 5] (important for FCC design) may be now enabled on top of any reference physics list via new UI commands. Existing physics list commands were also reviewed and the new set for GEANT4 10.3 is:

- */physics_list/em/SyncRadiation true,false*
- */physics_list/em/SyncRadiationAll true,false*
- */physics_list/em/GammaToMuons true,false*
- */physics_list/em/PositronToMuons true,false*
- */physics_list/em/PositronToHadrons true,false*

3. Model developments

More accurate simulation of EM shower profiles for LHC experiments requires review and improvements on the part per thousand level. This is important for high statistics analysis and other applications.

3.1. Bremsstrahlung: improved implementation of the LPM effect

Gamma emission for electron and positron bremsstrahlung [6] has been reviewed, with a focus on the Landau-Pomeranchuk-Migdal (LPM) effect. The LPM model is now fully consistent with the Migdal model, and there is an improved agreement between simulation and data, as can be seen in figure 1. Results with GEANT4 version 10.3.beta are in good agreement with measurements. This improvement results in a slightly narrower EM shower, but changes in results of full simulations are difficult to observe. For example, the R_9 distribution (the ratio of energy deposition in a crystal matrix $R_9 = E_{3x3}/E_{5x5}$) for CMS-type crystal calorimeter is practically unchanged.

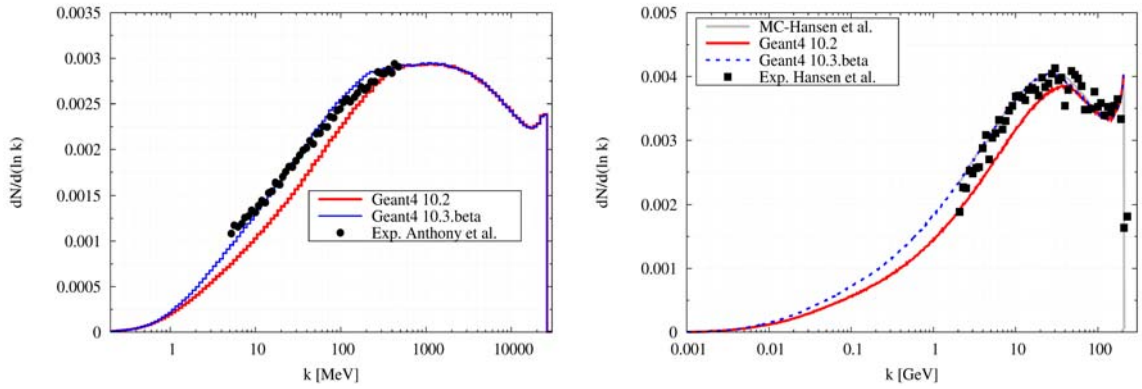

Figure 1. Number of photons produced per energy bin for 25 GeV e^- incident on a 0.15 mm thick Pb target (left), and 207 GeV e^- incident on a 0.128 mm thick Ir target (right). Points - data [7, 8], lines - GEANT4 simulation.

3.2. Multiple and single scattering

In recent years, models of single and multiple scattering have been under heavy development [9]. As a result, the following combination of models has been used as the default since GEANT4 10.0 [10]:

- for e^+/e^- below 100 MeV: the Urban model of multiple scattering [9];
- for e^+/e^- above 100 MeV, and protons, anti-protons, muons, pions, and kaons at all energies: a combination of *G4WentzelVIModel* of multiple scattering for small angles and *G4eSingleScatteringModel* single scattering model for large angles (WVI-SS);
- for all other charged particles: the Urban model.

The limit angle between multiple and single scattering (SS) is computed dynamically. It depends on the momentum of the particle and step size. This configuration works well for several multiple scattering benchmarks, but accurate simulation of low-energy electrons requires too many steps in vicinity of geometry boundary. In order to improve precision and CPU performance of electron transport, development of the *G4GoudsmitSaundersonMscModel* (GS) was initiated [11].

Implementation of GS was reviewed and rewritten for GEANT4 10.2. The model is a combination of the Goudsmit-Saunderson multiple scattering theory [12] with Rutherford differential cross sections, implemented according to the Kawrakow-Bielejaw [13, 14] hybrid model. Probability density functions (PDFs) are pre-computed on a two-dimensional grid, and a variable transformation is used to create smooth PDFs. This leads to accurate and robust sampling. The range factor used to limit the step length can be set to any value, with 0.2 as

the default, because the true step length is limited to the first transport mean free path [13, 14]. Boundaries are only reached in single scattering mode. The physics accuracy of GS is on the same level as the default Urban model. This can be seen in various validation tests, in particular, electron scattering in thin foils, energy deposit versus depth for low energy electrons, and the high energy calorimeter response. Computation times are similar to, or better than, those with the Urban model. The main advantage of GS compared to the Urban model is that the GS model is theory-based and hence does not have tuned parameters.

Figure 2 shows that the updated GS model for heavy media is comparable in accuracy to WVI-SS and the single scattering model (SS). The GS curve is closer to the data than the data for the Opt3 configuration, which is implemented in the *G4EmStandardPhysics_option3* EM physics constructor using the Urban model for all particles and a strict limitation on the step size. The accuracy of the current default Opt0 configuration is lower, but Opt0 requires a factor of approximately two times fewer CPU cycles compared to the GS and Opt3 in this case. The WVI-SS combination is not optimised for low energy electron transport, so it provides accurate results here, but is slower than the other models with this geometry. Recently, results

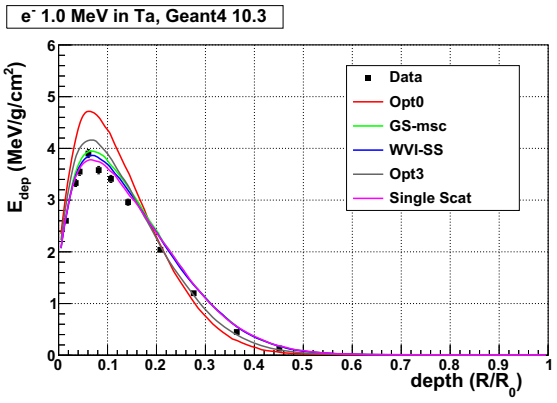

Figure 2. Dose deposit as a function of normalized depth for 1 MeV e^- incident on Ta for GEANT4 version 10.3, for different EM physics lists compared to measured data [15].

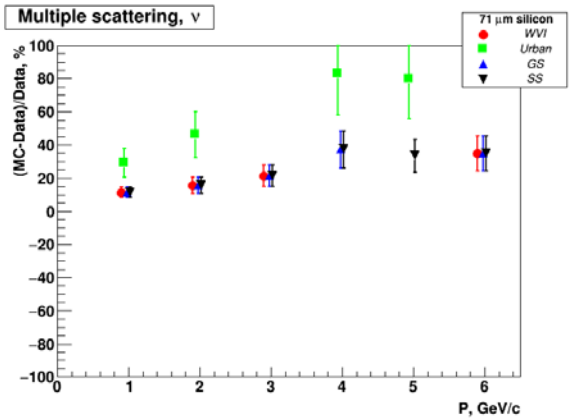

Figure 3. Simulation versus data [16] for the parameter ν of the Student's t fit function [16] for scattering of e^- off 71 μm Si as a function of beam momentum.

of measurements and simulations for few GeV e^- beam scattering in thin silicon layers were published [16]. In this work, a custom physics list with only the Urban model for multiple scattering was used. We repeated the same procedure as described in the manuscript and confirm that the tail parameter of the Student's t fit obtained with the Urban model does not agree well with the data (figure 3). At the same time, GS, SS and WVI models are in better agreement with measurement.

3.3. Nuclear form-factor parameterisation

The differential cross section of EM processes includes a nuclear form factor (FF) accounting for the spatial distribution of charge density. Until now, all scattering models used an exponential charge distribution for the form factor. In GEANT4 version 10.3, the form factor may be either exponential, Gaussian, flat, or none. The form factor may be selected using the new UI command

- */process/em/setNuclearFormFactor FF_type*
- *FF_type = None,Exponential,Gaussian,Flat*

Now any GEANT4 model may use this form factor for cross section computation and/or sampling of final state. In particular, these types are used in the current GEANT4 default physics configurations WVI-SS.

The new single scattering class *G4eSingleCoulombScatteringModel* (ESS) implements the screened relativistic treatment [17, 18] of the Mott cross section for electrons incident on a nucleus. This treatment accounts for effects due to the screened Coulomb fields, and finite sizes and rest masses of nuclei. Note that the Mott corrections are not taken into account in the default GEANT4 models. The calculation of the scattering parameters is performed in the center of mass system and Lorentz transformations are applied to obtain the energy and momentum quantities in the laboratory system after scattering. The differential cross section [17, 19] is given by:

$$\frac{d\sigma(\theta)}{d\Omega} = \left(\frac{Ze^2}{\mu c^2 \beta^2 \gamma}\right)^2 \frac{R_{Mott}|F_N(q)|^2}{(2A_s + 2\sin^2(\theta/2))^2}. \quad (1)$$

where Z is the atomic number of the target nucleus, $\mu = m\frac{Mc^2}{E_{cm}}$ is the relativistic reduced mass of the system, m and M are rest masses of the electron and of the target nuclei respectively, and E_{cm} is the total center of mass energy; A_s is the screening coefficient [20]; R_{Mott} is the ratio of the Mott to Rutherford differential cross section obtained by an analytical fit [21]; $F_N(q)$ is the nuclear form factor. The importance of the form factor, especially at high scattering angles, is shown in figure 4. This model, with the factorization of the screening term, is suitable for

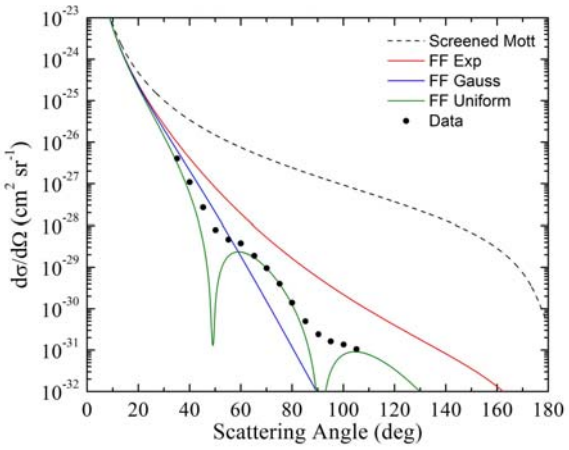

Figure 4. Differential cross section as a function of the scattering angle for 183 MeV electrons in indium. Points are data [22], lines are simulation with different form factor options: none - black, exponential - red, Gaussian - blue, flat - green.

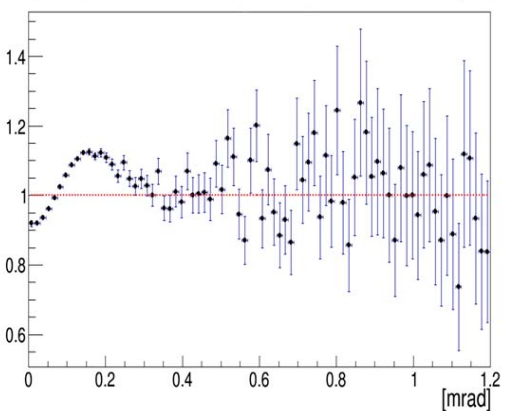

Figure 5. The ratio for distributions of scattering angle of 10 GeV muon scattered of 300 μm silicon target for the two single scattering models described in the text. The difference is visible only in the central part of distributions.

incident electrons with energy above 200 keV. Screening and spin effects are treated separately in Equation 1. Zeitler and Olsen [23] suggested that for electron energies above 200 keV the overlap of spin and screening effects is small for all elements and for all energies; for lower energies the overlapping of the spin and screening effects may be appreciable for heavy elements and large angles.

The ESS class allows calculation of the nuclear stopping power, non-ionizing energy loss (NIEL), the scattered direction of the outgoing particle, and the energy transferred to the target atom of the material. If the transferred energy is greater than the threshold energy needed to

displace an atom, a secondary recoil ion is generated. In the user analysis, the kinetic energy of the secondary particles may be multiplied by the Norgett-Robinson-Torrens expression [24, 25] that approximates the Lindhard partition function to obtain the NIEL deposited in the target material; moreover nuclear stopping power may be computed.

3.4. Relativistic corrections for muon scattering

For scattering of high energy charged particles, nuclear recoil may be important. Figure 5 presents the results of simulation of muon scattering in a thin silicon layer with the default SS model and an alternative *G4hCoulombScatteringModel* for simulation of muon scattering in silicon. The new model uses the same approach [17] to describe two-body scattering as the single scattering model discussed in the previous sub-section. The effect of relativistic corrections may be better identified in the ratio of two distributions, where it is seen that corrections affect mainly the central part of the angular distribution. This study confirms that for high energy simulation it is enough to add relativistic corrections to the default models instead of creating dedicated models.

3.5. Low energy models

Initialisation of the atomic de-excitation module was revised and several new options were added. In particular, the possibilities of simulating full Auger cascades, full gamma cascades, and using alternative data [26] for fluorescence lines are available [27]. New UI commands can be used on top of any reference physics list:

- */process/em/augerCascade true,false*
- */process/em/fluoBearden true,false*
- */process/em/deexcitationIgnoreCut true,false*

Extensive developments were carried out for the simulation of radiation effects at the cellular level (Geant4 DNA). New models were added and software infrastructure was extended. One of the most significant developments was the addition of discrete electron transport models for gold [28]. Alterations were made to the software infrastructure which has now opened the possibility of using standard and DNA models simultaneously.

4. New validation results

Validation of EM physics is a continuous Geant4 task [29]. In this work we report only few selected results but the full set of EM benchmarking is available in the Geant4 web pages.

Electron multiple scattering is validated at 13 and 20 MeV by comparison of simulations to a thin foil transmission benchmark [30]. One comparison is the width of the central Gaussian peak measured 1.2 m from the foil. Figure 6 shows the ratio of simulated to measured peak widths at 13 MeV for each scattering target, using Geant4 version 10.2.patch2. The accuracy of the experiments was quoted as $\pm 1\%$ for the width of the central peak for each sample. Results with the Urban model are typically within 2% of the measured values. The GS model shows larger discrepancies of up to 6% for the C target. Typically, the central peak widths in the GS simulations are narrower than measured.

The shapes of the distributions for different models are slightly different. The maximum deviation of the shape may be estimated by plotting the ratio of the simulation curve versus measured data, as shown in figure 7 for three scattering models for a titanium foil at 20 MeV. The titanium foils, along with beryllium and carbon, show the poorest agreement; for the other foils the agreement is better. For the titanium foil, both GS and SS predict more fluence in the central region than the measurement, and less fluence in the tails. In contrast, the Urban model predicts less fluence in the central region, and more in the tails. Overall, the Urban results

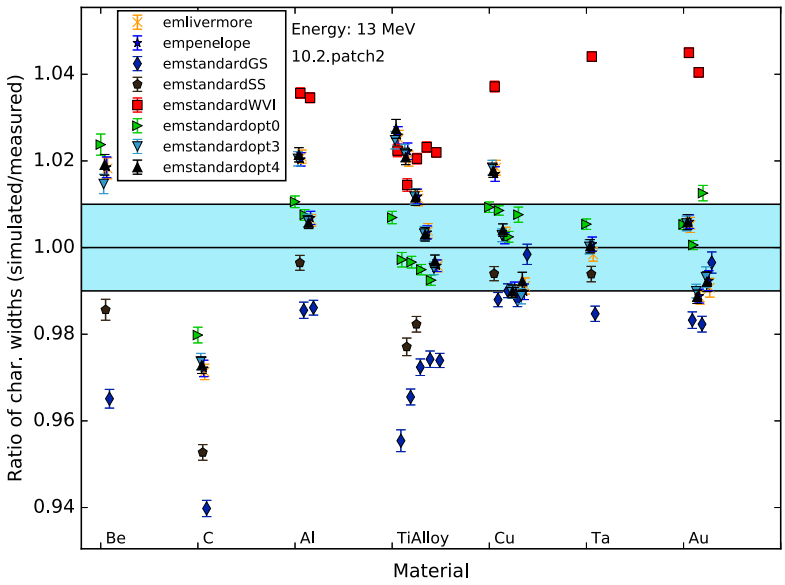

Figure 6. The ratio of the simulated to measured characteristic widths [30] of the central peak of the scattered 13 MeV e^- beam for different scattering targets and physics lists.

are in better agreement with the measured data than the GS results are, and the GS results are in better agreement with SS. The theory-based SS and GS models use similar screened Rutherford elastic cross sections, so their shapes are close to each other but with a difference from measurement of 6–8% at small and large angles. Improvement of these shapes could be achieved by taking Mott corrections into account. The Urban model was tuned to these data and correspondingly shows the smallest deviation.

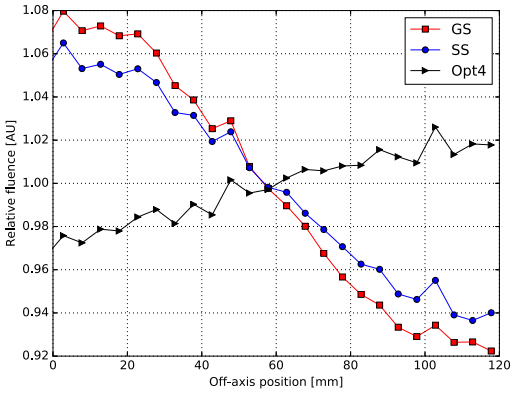

Figure 7. Ratio of the simulated fluence to measured fluence for the 82.4 μm thick Ti alloy target as a function of distance from the central axis.

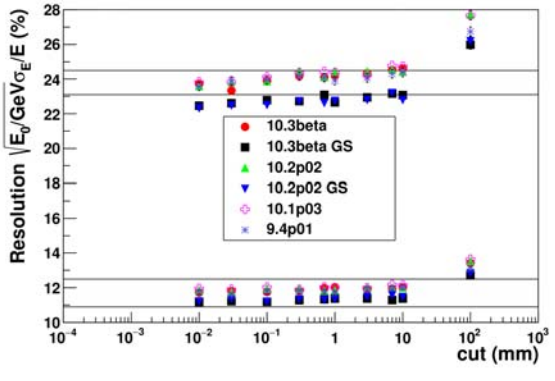

Figure 8. e^- 10 GeV in Pb/Scin sampling calorimeters: points are simulation with different GEANT4 versions; bands are one standard deviations uncertainty of data [31], [32].

The electromagnetic shower simulation is stable throughout recent GEANT4 versions at a

level well below 1%. In particular, energy resolution is practically unchanged and agrees with the data within experimental uncertainty (figure 8). In this plot, measured resolutions of two lead/scintillator sampling calorimeters as a function of range cut are shown for the default EM physics and for the case when GS is used for simulation of e^+, e^- multiple scattering below 100 MeV. The results with GS are competitive for the high sampling fraction calorimeter. For the low sampling fraction calorimeter, the resolution obtained with GS is lower than measurements.

5. Conclusions

GEANT4 EM sub-libraries were updated for versions 10.2 and 10.3. The main improvements introduced were for multiple and single scattering models. A new implementation of the Goudsmit-Saunderson multiple scattering model was shown to be competitive with the Urban model for low-energy electron transport. At the same time, overall validation results confirm the choice of the Urban model as a default for the electron and positron transport simulation below 100 MeV. Improvements to models of nuclear form factors, muon scattering, bremsstrahlung, and atomic de-excitation were also made. EM shower shapes are stable with these changes. The upper energy limit for GEANT4 EM physics was extended from 10 to 100 TeV. The definition of the physics per geometry region may now be done via the new UI commands.

References

[1] Agostinelli S et al. 2003 *Nucl. Instrum. Meth. A* **506** 250-303
[2] Allison J et al. 2016 *Nucl. Instrum. Meth. Phys. Res. A* **835** 186-225
[3] Bernal M A et al. 2015 *Phys. Med.* **31** 861-74
[4] Bogdanov A G et al. 2006 *IEEE Trans. Nucl. Sci.* **53** 513-9
[5] Apostolakis J et al. 2015 *J. Phys: Conf. Ser.* **664** 072021
[6] Allison J et al. 2012 *J. Phys.: Conf. Ser.* **396** 022013
[7] Anthony P L et al. 1997 *Phys. Rev. D* **56** 1373
[8] Hansen H D et al. 2004 *Phys. Rev. D* **69** 032001
[9] Ivanchenko V N, Kadri O, Maire M and Urban L 2010 *J. Phys.: Conf. Ser.* **219** 032045
[10] Ivanchenko V N et al. 2014 *J. Phys.: Conf. Ser.* **513** 022015
[11] Kadri O, Ivanchenko V, Gharbi F and Trabelsi A 2009 *Nucl. Instrum. Meth. B* **267** 3624-32
[12] Goudsmit S and Saunderson J L 1940 *Phys. Rev.* **57** 24
[13] Bielajew A F 1996 *Nucl. Instrum. Meth. Phys. Res. B* **111** 195
[14] Kawrakow I and Bielajew A F 1998 *Nucl. Instrum. Meth. Phys. Res. B* **134** 325
[15] Lockwood G J et al. 1987 Calorimetric Measurement of Electron Energy Deposition in Extended Media– Theory vs. Experiment *SANDIA REPORT SAND79-0414.UC-34a*
[16] Berger N et al. 2014 *JINST* **9** P07007
[17] Boschini M J et al. 2011 *Proc. 13th ICATPP Conf.* (World Scientific, Singapore) 961-82 *ISBN: 978-981-4405-06-5*
[18] Boschini M J, Rancoita P G and Tacconi M 2016 SR-NIEL Calculator: http://www.sr-niel.org/
[19] Leroy C and Rancoita P G 2016 Principles of Radiation Interaction in Matter and Detection (4th Ed.) (World Scientific, Singapore) *ISBN-978-981-4603-18-8* (printed); *ISBN.978-981-4603-19-5* (ebook)
[20] Molière G 1947 *Z. Naturforsh A* **2** 133-45; **3** 78
[21] Boschini M J et al. 2013 *Rad. Phys. Chem.* **90** 39-66
[22] Hahn B et al. 1956 *Phys. Rev.* **101** 1131
[23] Zeitler E and Olsen A 1956 *Phys. Rev.* **136** A1546-52
[24] Jun I 2001 *IEEE Trans. Nucl. Sci.* **48** 16275
[25] Messenger S R et al. 2003 *IEEE Trans. Nucl. Sci.* **50** 1919-23
[26] Bearden J A 1967 *Rev. Mod. Phys.* **39** 78
[27] Incerti S et al. 2016 *Nucl. Inst. Meth. B* **372** 91-101
[28] Sakata D et al. 2016 *J. Appl. Phys.* **120** 244901
[29] Apostolakis J et al. 2010 *J. Phys: Conf. Ser.* **219** 032044
[30] Ross C K, McEwen M R, McDonald A F, Cojocaru C D and Faddegon B A 2008 *Med. Phys.* **35** 4121
[31] Bernardi E et al. 1987 *Nucl. Inst. Meth. A* **262** 229-42
[32] D'Agostini G et al. 1989 *Nucl. Inst. Meth. A* **274** 134-44